Testing of Image Segmentation Methods

I.V.GRIBKOV, P.P.KOLTSOV, N.V.KOTOVICH, A.A. KRAVCHENKO, A.S.KOUTSAEV,
A.S. OSIPOV, A.V. ZAKHAROV
Scientific Research Institute for System Studies, Russian Academy of Sciences (NIISI RAN)
Nakhimovskii pr. 36-1, Moscow, 117218 RUSSIAN FEDERATION
vokbirg@yauza.ru, koltsov@niisi.msk.ru

Abstract: Digital image segmentation is broadly used in various image processing tasks. A large amount of image segmentation methods gives rise to the problem of of method's choice, most adequate for practical purposes. In this paper, we develop an approach which allows quantitative and qualitative estimation of segmentation programs. It consists in modeling both difficult and typical situations in image segmentation tasks using special sets of artificial test images. The description of test images and testing procedures are given. Our approach clears up specific features and applicability limits of four segmentation methods under examination.

Key-Words: - image processing, energy minimization, image segmentation, ground truth, testing, performance evaluation.

1 Introduction

As one can find a lot of definitions for the term "image segmentation" (for example, [1] – [4]), we give our *ad hoc* definition. We consider segmentation as image dividing into nonintersecting connected domains, so that each domain contains whole object or its part. Such an approach to segmentation defines a non-empty class of real images in natural environment, when segmentation is applicable for detection purposes. For example, air-space photos [5], images in computer diagnostic of some diseases [6] belong to this class. In many cases, the similarity of objects' elements is higher than their similarity comparative to adjacent background or neighboring objects [3]. This observation gives raise for a number of computer-aided methods for image segmentation. The joint methodological basis for these methods is search and detection of homogeneous (in some sense) domains. Usually these domains are built up in accordance with their contrast level, color, texture filling, etc.

Nowadays there exists a considerable amount of literature on segmentation methods (for example, [1]-[9]). Lots of computer segmentation programs can be found in the Internet [12]-[15]. Most of the methods perform image segmentation by solving some optimization problem with different types of functionals to be minimized [2],[3],[7].

For brevity, we will call "*segmentators*" both analytic methods for image segmentation, and program realizations of these methods.

It is obvious that different segmentators provide different solutions of the problem. Our testing has to clear up the question about methods' quality in solving of various segmentation tasks. Also, our testing should help to choose the most adequate method.

In this paper we study some properties of four segmentators with the aid of our PICASSO (PICture Algorithms Study Software, [10],[11]) program system. PICASSO's datasase accumulates artificial image samples both typical for the real images and difficult for prosessing by image processing methods. Like in the PICASSO general approach, the comparative study of operating quality of segmentation methods is fulfiled using artificial test images under supervised distortions and with known true segmentation.

Certainly, the definition of what is difficult and what is typical here is non formal but speculative problem. Usually the problems of that type are considered as badly formalized. Conventional approach for solving such problems is resort to the investigator's experience. An artificial test image set is the result of analysis of a large amount of segmentations by means of different methods. Such a set should provide certain completeness of difficult and typical situations. Of course, the test image set should be supplied with proper procedures for quantitative evaluation of the segmentators under testing. The behavior of segmentators on these images allows evaluating methods' properties and efficiency.

The structure of this article is as follows.

In Section 2 we introduce basic notions which we use in the article.

In Section 3 we briefly describe four methods for image segmentation. These methods will be tested in Section 5.

In Section 4 we describe artificial test image sets that model difficult situations for segmentators. Also we show some examples of segmentation and give methods for measurement of segmentation results.

Section 5 contains results of our testing as well as brief explanation of these results.

Section 6 is a concluding one.

2 Basic Notions in Segmentation

Basic notions in image segmentation are segment, region, segmentation map and boundaries. A segmentation program produces a new image – a segmentation map - containing domains of uniform filling. If initial grayscale image has many intensity gradations (for example, 256), in a typical case the resulting segmentation map has essentially smaller number of intensity gradations (for example, 3-5). The homogenous areas on the segmentation map are referred to as segments. Note that the boundaries between segments can be found very easily. After imposing of the segmentation map onto the initial image, the boundaries of the segments contour areas on the initial image. These areas are called regions. Segmentation is calculation of a segmentation map and partitioning of the initial image into regions.

Let's illustrate the basic notions of segmentation on example of processing of an image using JSEG segmentator [9]. Hereinafter JSEG will be tested alongside with the three other segmentators.

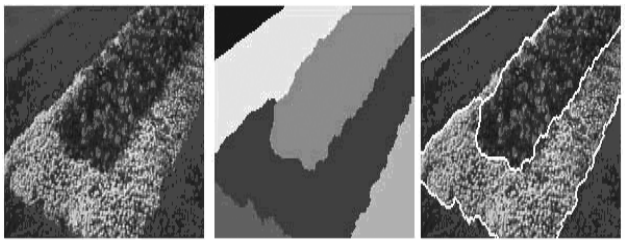

Fig.1. *Example of image segmentation (citation from [9]): a) – initial image, b) – segmentation map, c) – initial image with regions and boundaries*

The initial image (a flowerbed) is shown on Fig.1a. The segmentation map is shown on Fig.1b, where we can see homogenous segments. Areas of the initial image on Fig.1a, corresponding to segments on Fig.1b, are regions. By definition, the boundaries of segments are boundaries of regions. On Fig.1c, the boundaries are imposed on the initial image.

The number of segments obtained depends on specific features of a segmentator. In simple segmentation methods, the number of segments should be preset manually. Some methods provide upper bound for the number of segments. In other more complex programs, optimal number of segments can be calculated automatically.

Common feature of all segmentators we consider is creation of a segmentation map derived from the initial image.

3 Segmentation Methods Tested

We have chosen four segmentators for testing: JSEG [9],[12], EDISON [7],[13], EDGEFLOW [2], [14], MULTISCALE [8],[15]. These segmentation methods are well known and often used for image segmentation purposes. Most of these methods have several control parameters. Some parameters specify image size or output format. Other parameters are essential for the segmentation process.

3.1. JSEG segmentator

This method [9] is aimed to segment images and video, containing monochrome or color regions.

If the parameters of JSEG are not specified, the program is able to establish them automatically. Therefore, we did not set essential parameters at all while testing JSEG.

3.2 EDISON segmentator

EDISON program system [7] implements image segmentation, boundaries extraction and noise filtration.

One of the main parameters of EDISON is the minimal size (in pixels) of a region which this method can create. For testing, we used two values of this parameter: 100 and 1000. Accordingly, we denote two instances of this method as EDISON 100 and EDISON 1000. Other parameters have the same values that the authors used in their examples [7].

3.3 EDGEFLOW segmentator

In this method [2], a well-known edge flow approach is applied for image segmentation and boundary detection.

EDGEFLOW method has an essential "offset" parameter. We consider two "offset" values: 10 and 26. Further on, we denote two instances of this method as EDGEFLOW 10 and EDGEFLOW 26.

3.4 MULTISCALE segmentator

While processing by MULTISCALE segmentation method [8], an image first is analyzed in coarser scale, and then in finer scale.

In [8], some parameters are recommended as "safe". These values have been taken at testing.

4 Artificial Image Sets, Examples of Segmentation and Testing Approaches

After analysis of a large amount of segmentations, we have chosen the following difficult situations for segmentators:

- segmentation of domains with slowly varying intensity (i.e. brightness);
- segmentation of angles on images;
- segmentation of low contrast images;
- segmentation of noisy and blurred images.

Test image sets described in the present section, model these difficult situations and allow numerical evaluating of segmentation quality.

All the images are of 256x256 pixels in size. Their intensity ranges from 0 to 255 units. In order to analyze the results of segmentation, we use several techniques described below.

Analysis of segmentation results is a special problem. Segmentators can create both monochrome and color segmentation maps. Moreover, different segmentators use different fillings of the segments. The intensity and color that a program uses to fill in the segments are conventional and usually have no relation to intensity and color of the original image. Even after blurring or noising of initial image, a segmentator can change filling of corresponding segments. Evidently, the boundaries are sets of pixels which do not depend on the color or filling. Therefore the boundaries are more convenient for comparison. So we prefer to compare not segments, but their boundaries. Hereafter we use only boundaries of segments for calculations of the segmentation quality.

4.1 Segmentation of domains with slowly varying intensity

Proper segmentation of images containing domains with slowly varying intensity is proved to be a hard task for all segmentators we have tested.

Fig.2 presents examples from a one-parametric family of images with slow intensity variation.

Here the intensity is constant along the vertical direction and linearly increases along the horizontal one. On the left margin of all images, the intensity is zero. On the right margin, the intensity is equal to some value b that is the parameter of the family. The values of b are integers ranging from 0 to 255.

Correct segmentation of such an image should result in one segment with no boundary lines at all. But the practice exposes that in domains of slow intensity variance, the segmentators do create some "false" segments. Their boundaries are traditionally called "false boundaries".

Fig.2. *Intensity at the right: a) 0, b) 200, c) 255. Intensity at the left: 0 anywhere.*

Fig.3 shows an example of segmentation of three images. The segments are omitted, only the boundaries between segments are presented. Here the intensity linearly increases from 0 at the left margin up to 10, 100, 200 respectively at the right margin.

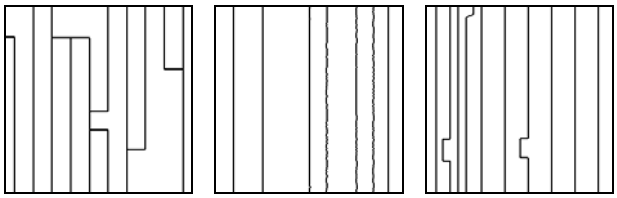

Fig.3. *EDGEFLOW 10 method. Segmentation of domains with slowly varying intensity*

4.1.1. Testing approach

The number of boundary points $n(b)$ depends on the top intensity at the right margin of the test image. The evaluation of the segmentation quality using the images on Fig.2, consists in counting of the number of boundary points $n(b)$ between resulting segments. Before computations, all boundary lines in all segmented images are reduced to one-pixel width.

Therefore, the number of points in "false boundaries" is chosen as a criterion for evaluation for this series of images. The lower is the number of boundary points $n(b)$, the better is the quality of segmentation.

After this, the dependencies $n(b)$ are used to get smooth trend curves. An example is shown on Fig.4. Trend curve is (usually, polynomial) approximation of a plot. It is computed by standard means. Thus $n(b)$ can be thought of as consisting of noisy behavior around a smooth trend curve. The trend curves are necessary because the plots of $n(b)$ are scattered and difficult for analysis. This means certain instability of segmentation: small changes of an image may cause significant changes of the segmentation results. As it can be seen on Fig.3,4 if the maximal intensity of the images increases, then

the number of "false boundaries" may either increase or decrease abruptly within some limits. Similar effects can be seen for the segmentation of angles, as well as for noisy and blurred images. An example of segmentation of angles is given below on Fig.6. However, despite the presence of salient points, the plot of segmentation of angles (Fig.13) exposes a tendency to a more exact segmentation when the angle value increases. Such tendencies can be made more apparent by use of the trend curves. In Section 5, the trend curves are presented on all plots, except for Fig.13, 14.

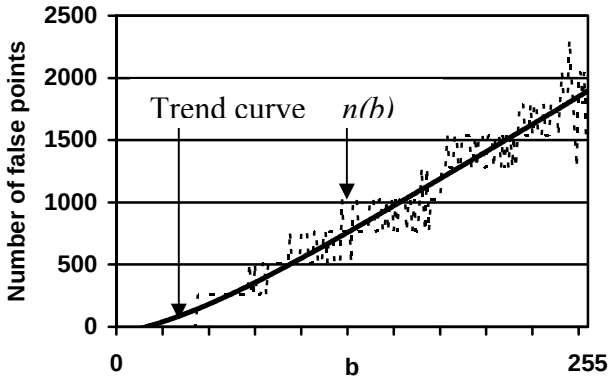

Fig.4. *Example of original plot of n(b) and its trend curve (JSEG method)*

Comparative results of testing are described in subsection 5.1.

4.2 Segmentation of angles on images

Correct preservation of angles is another difficult task for segmentators.

Fig.5 presents examples of a one-parametrical duotone image family that consists of 180 images. The parameter is the angle value, from 1 to 180 degrees.

a) b) c)

Fig.5. *Angles: a) 2, b) 80, c) 160 degrees. Image intensity is 50, background intensity is 200*

Here we test the ability of segmentators to preserve the vertex of an acute angle in the segmented region. Good segmentation should result in an image of the same geometry and, maybe, different coloring/filling. However, the experiments show that some methods make the vertex round. The general tendency is that obtuse angles are preserved well, and acute angles are often distorted. The smaller is the angle, the greater is the distortion.

As an example, on Fig.6 we show boundaries obtained after segmenting images from the family on Fig.5. Angle values are 5, 30, 90 degrees.

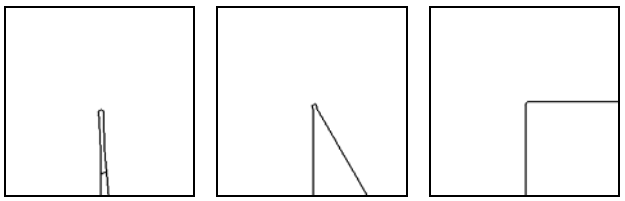

Fig.6. *JSEG method. Angle segmentation*

The measurements show that variations of foreground and background intensities have no significant effect on the result. Therefore these intensities were taken same as presented on Fig.5 and remained constant during testing.

4.2.1. Testing approach

The distance *d* between the exact vertex position and the nearest point of the obtained angle segment was chosen to be a criterion for evaluating the quality of segmentation (Fig.7).

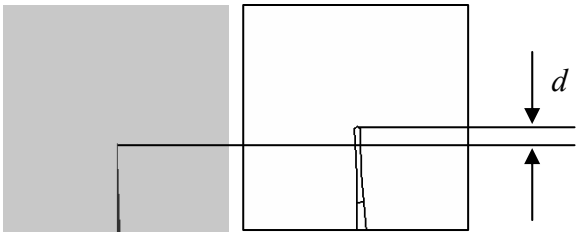

Fig.7. *Result of an acute angle segmentation*

The smaller is *d*, the better is segmentation quality. The dependence of this distance on the angle value can be displayed on a plot.

Comparative results of testing are described in subsection 5.2.

4.3 Segmentation of low contrast images

Segmentation of low contrast images is also difficult for some segmentators.

Examples from two-parametrical family of duotone images are presented on Fig.8. The object (a circle, radius 100 pixels) is located in a square with background filling.

Background and circle intensities are parameters of the family. An object (a circle) is detected after segmentation as a separate segment if there is sufficient difference between intensities of the object and background. An object is also confidently

found out in case of greater intensity difference. But if the intensities of background and object are very close, such an object cannot be detected and resulting segmented image proves to be empty.

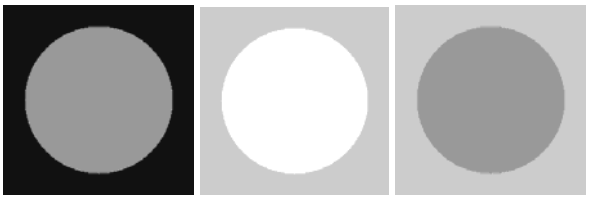

Fig.8. C*ircles of intensity a) 150 on background intensity 30, b) 255 on 200, c) 150 on 200*

4.3.1. Testing approach

Let background intensity be x, circle intensity be $x+y$. Minimal value $y(x)$ for correctly segmented circle can be found for each given background intensity x. We call the dependence $y(x)$ "difference threshold" between intensity values x and $x+y$. Thus the value $y(x)$ can be represented graphically. This dependence shows sensitivity of segmentators for detecting non-contrast objects.

The results of testing are described in subsection 5.3.

4.4 Segmentation of noisy and blurred images

Noisy and blurred images are traditionally difficult for processing.

In order to evaluate the segmentation of noisy and blurred images, we use 6 initial images, which are divided into 2 groups: "simple" and "complex" images.

Simple images:

Circle (Fig.8), radius 100 pixels, foreground intensity 200, background intensity 30

Angle (Fig.5), value 110°, foreground intensity 50, background intensity 200.

Segmentation of these images is very easy, as each image is contrast enough and includes large homogenous areas.

Complex images:

Step, Junction, Snail, Roof (Fig.9).

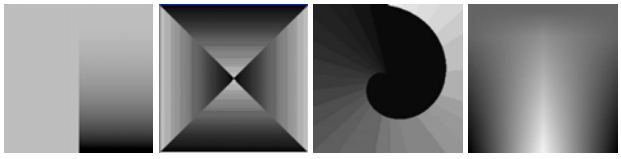

Fig.9. "*Complex*" *images Step, Junction, Snail, Roof*

Complex images were already used in other testing problems [10]. They include domains with slowly varying intensity, angles and low contrast areas. Some examples of segmentation are shown on Fig.10. Only boundaries of segments are presented.

Each of these 6 initial test images generates two sets of test images. First set is obtained by adding Gaussian noise to the image. Second set is obtained by Gaussian blurring of the initial image.

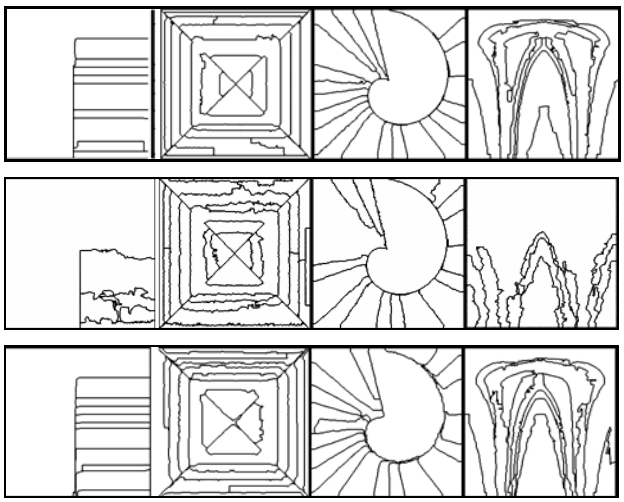

Fig.10. EDISON 1000 method. Top row: segmentation of initial images Step, Junction, Snail and Roof. Middle row: Gaussian noising, deviation 4. Bottom row: Gaussian blurring, radius 3 pixels.

Segmentation of Step, Junction, Snail and Roof is difficult for all methods. One can see on Fig.10 (top row) that segmentation of even initial images causes "false boundaries". The presence of domains with slowly varying intensity considerably changes the behavior of segmentators comparative to their behavior on simple images. Due to this, in Section 5 (subsections 5.4 and 5.5) we show separate plots for simple images and for complex images.

4.4.1. Testing approach

Let I be an initial test image and I_σ be the image created by adding Gaussian noise with deviation σ. Thus $I_0=I$. Denote $s(I_\sigma)$ - the result of segmentation of I_σ and $B(s(I_\sigma))$ – the boundaries of segments on $s(I_\sigma)$. An example of such boundaries is shown on Fig.10, middle row.

In order to estimate the results of segmentation, we find distances between $B(s(I_\sigma))$ and the "ground truth"- true boundaries $B(I)$. Here $B(I)$ is special image containing boundaries of the initial image.

If I is a simple image (Circle or Angle), B (I) contains *a priori* set boundaries and is taken from the PICASSO's database. Such boundaries can be built manually. Therefore, B (I) is the same for all segmentators. The boundaries are self-evident and therefore are not depicted here.

In case of complex images (Fig.9), comparison of $B(s(I_\sigma))$ with manually built ideal "ground truth" boundaries is senseless. So we take $B(I) = B(s(I_0))$ - the result of segmentation of the initial image $I_0=I$. Therefore, $B(I)$ is special for each segmentator. An example of such $B(I)$ is shown on Fig.10, top row.

For blurring, Gaussian blur radius r is taken instead of noise deviation σ.

Numerical estimation of segmentation quality includes two steps: a) measurement of segmentation results; b) averaging of measurement data. This results in a plot for each method.

4.4.2. Measurement of segmentation results

In order to measure distances between curves, we use Hausdorff distance $\chi(\sigma)= \chi(\ B(I),\ B(s(I_\sigma))\ )$ and also "mean" distance $\mu(\sigma)= \mu(\ B(I),\ B(s(I_\sigma))\ )$.

Classical Hausdorff distance measure $\chi(X,\ Y)$ between two point sets X and Y is defined as

$$\chi(X,Y) = \max\left[\max_{x\in X}\rho(x,Y), \max_{y\in Y}\rho(y,X)\right].$$

This distance measure is not always optimal, but it is well-known and commonly used. Mean distance is defined as

$$\mu(X,Y) = \frac{1}{2}\left[\frac{1}{N_X}\sum_{x\in X}\rho(x,Y) + \frac{1}{N_Y}\sum_{y\in Y}\rho(y,X)\right].$$

Here $\rho(x,\ Y)$ is the distance from a point $x \in X$ to the set Y: $\rho(x,Y) = \min_{y\in Y}\rho(x,y)$, where $\rho(x,\ y)$ is Euclidian distance between points x and y. N_X and N_Y are numbers of points in X and Y. In our case, the sets X and Y are the sets of boundary points. So, both distances should be measured in pixels. An example is shown on Fig.11. Note that $\mu \le \chi$.

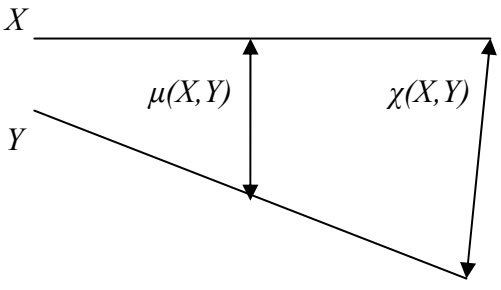

Fig.11 *Hausdorff and mean distances*

Simultaneous usage of distance measures χ and μ gives an opportunity of more precise analysis of segmentation results. Indeed, if both values $\chi(X,\ Y)$ and $\mu(X,\ Y)$ are small, then the boundaries X and Y are close to each other. If $\mu(X,\ Y)$.is small but $\chi(X,\ Y)$ is large, then it means that X contains some points remote from Y (or vice versa), but the number of such points is small. If both μ and χ are large, then the number of mutually remote points is large, so X and Y are considerably different.

4.4.3. Averaging of measurement data

For each segmentator: 1. The distances χ and μ are calculated separately for every test image set. 2. The distances χ and μ are averaged over chosen test images. 3. Trend curves are calculated using the averaged distances χ and μ.

5 Results

5.1 Segmentation of domains with slowly varying intensity

Segmentation of domains with slowly varying intensity (Fig.2) proved to be a hard task for all segmentators tested. All of them produce lots of false boundaries (Fig.3).

Fig.12 shows that the quantity of false boundary points ceases to increase and even decreases on reaching big enough value of parameter b (maximal intensity of gradient filling test image), for EDISON 100, 1000 and MULTISCALE segmentators. As EDISON and MULTISCALE process acute angles well (see Fig.13), we suppose that their application area is processing of high-contrast images, when good preservation of object's geometry is necessary.

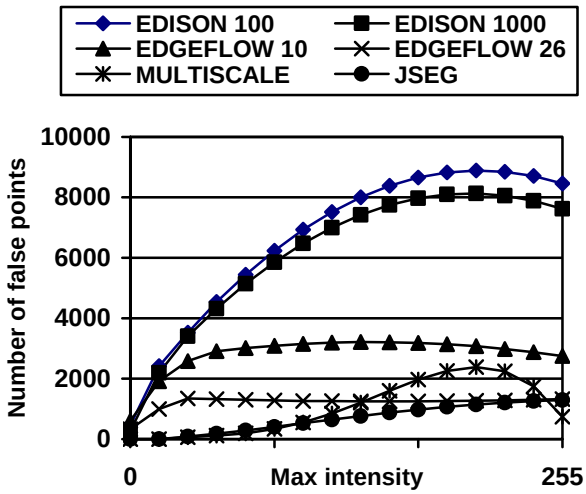

Fig.12. *Number of false boundary points depending on maximal intensity of test images.*

As to EDGEFLOW 10 and 26, the number of false points only slightly depends on the maximum intensity of the image. However, as one can see on Fig.3,4, segmentators are unstable – the number of false boundaries can depend on random factors.

5.2 Segmentation of angles on images

As it has turned out, EDISON and MULTISCALE segmentators perfectly preserve angles (Fig.5): the distance between true angle vertex and the corresponding point on segmented image always equals to 0-1 pixels. Therefore we don't show the testing results for these segmentation methods.

Conversely, both EDGEFLOW 26 and JSEG segmentators considerably distort acute angles (Fig.13). Distortions caused by EDGEFLOW and JSEG are of different type. Processing of small homogeneous regions (in particular, small angle segments) is difficult for EDGEFLOW. In such a case this segmentator creates false segments, which have no relation to the initial image. EDGEFLOW works better if an image contains objects large enough and the objects have "strong" boundaries. As to JSEG, it doesn't create false segments while segmenting homogeneous regions, but rounds off acute angles.

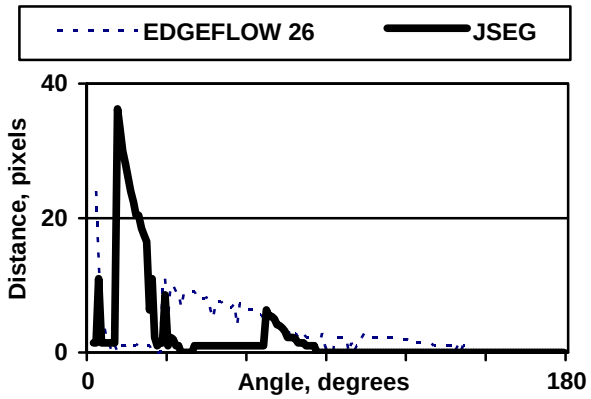

Fig.13. *Angle distortion after segmentation by EDGEFLOW 26 and JSEG methods*.

5.3 Segmentation of low contrast images

All segmentators but JSEG separate a circle (Fig.8) as a segment if the difference between object's intensity and background intensity is 1-2 units, regardless of whether object is brighter than background or vice versa.

Result of segmentation by JSEG depends on the background intensity value. Fig.14 demonstrates how the background intensity affects on a low contrast object separation by JSEG segmentator. The vertical axis of the plot shows the "difference threshold". This is the minimal exceedance of object's intensity over the background intensity necessary for correct segmentation of the test image. When the background intensity ranges from 0 to 15 (Fig.14), a circle is separated as a segment only if its intensity exceeds background intensity at least by 23 units. However, if background intensity value ranges from 22 to 255, a circle is separated as a segment if its intensity exceeds background intensity by 1 unit only.

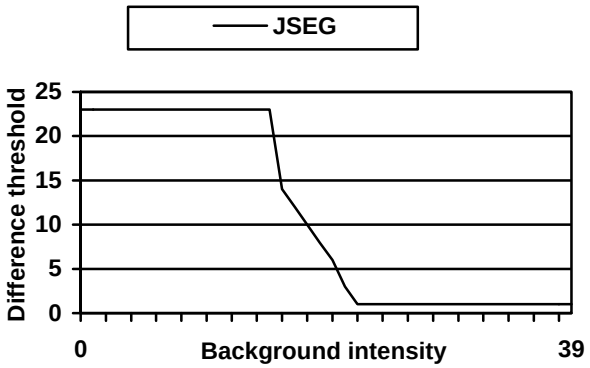

Fig.14. *Segmentation of low-contrast domains. JSEG method*

Perhaps, this feature is inherent only for the given program realization [12] of JSEG method. Such a feature of JSEG can be useful in some image recognition tasks. In many cases, it is important to distinguish bright objects primarily, whereas dark objects on a dark background are not significant. Human vision functions in a similar way.

5.4 Segmentation of noisy images

To evaluate the segmentation quality of the algorithms applied to the noisy images, we added Gaussian noise with standard deviation σ from 0 to 30 (with step 1) to the images on Fig.5,8,9.

Simple images. Fig.15 shows comparative results for all four methods. The segmentators are applied to Circle and Angle images (Fig.8,5). After segmentation, we compared the obtained curves with the "ground truth" boundary contours. Here and further we show trend curves which average the measurement results.

It is clear that JSEG displays better behavior than all other segmentators. It perfectly suppresses noise. Since the distances χ and μ between the boundary after segmentation and the "ground truth" are small, we may conclude that this segmentator well preserves the shape of the boundary contours.

As the noise deviation increases, the distances χ and μ also increase for all segmentators. However, note (Fig.15) that sometimes χ exceeds 50 pixels provided that the radius of the circle equals to 100 pixels. This means that the segmentation looses its connection with the original images and becomes improper. The decrease of some curves for large σ also points to this fact. We can conclude that EDISON can be used for the noise deviation values not greater than 15-20, and EDGEFLOW and MULTISCALE – for 3-5 only.

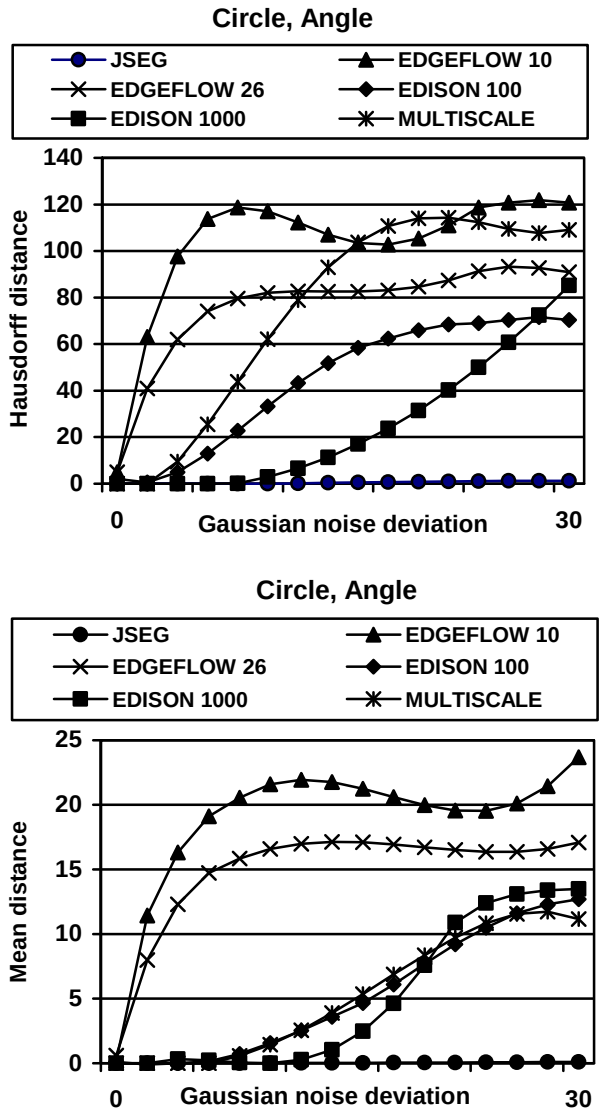

Fig.15. *Noisy images segmentation. Simple images. Averaged over Circle and Angle images*

Pay attention at the scales of the vertical axes of upper and lower plots on Fig.15. Hausdorff distance range is 0..140, while mean distance range is 0..25. This means that segmentators create many junk but little segments. Such an effect is best visible on simple images. An example is given on Fig.16.

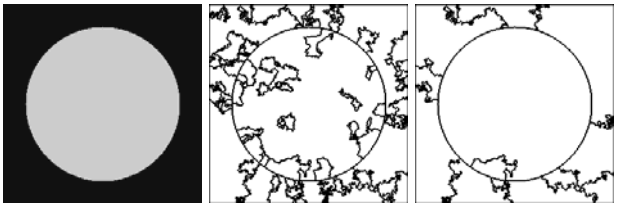

a b c

Fig. 16. *a) initial image, b) result of segmentation by EDISON 100, c) result of segmentation by EDISON 1000. Added noise with deviation σ=19*

Fig.16 can be explained in the following way. A segmentator takes a noise pattern on initial image for a separate region and hence creates separate junk segments. Thus, noise suppression capability of EDISON 1000 is better than that of EDISON 100.

Complex images. Fig 17 plots the results for all segmentators applied to the Step, Junction, Snail and Roof images (Fig.9). As we see, EDGEFLOW 26 produces the highest values of χ and μ. The plot starts to fall down for the values of σ equal to 7-8, which points to the large distortions during the segmentation. We conclude that it is the upper noise level for a correct application of this method.

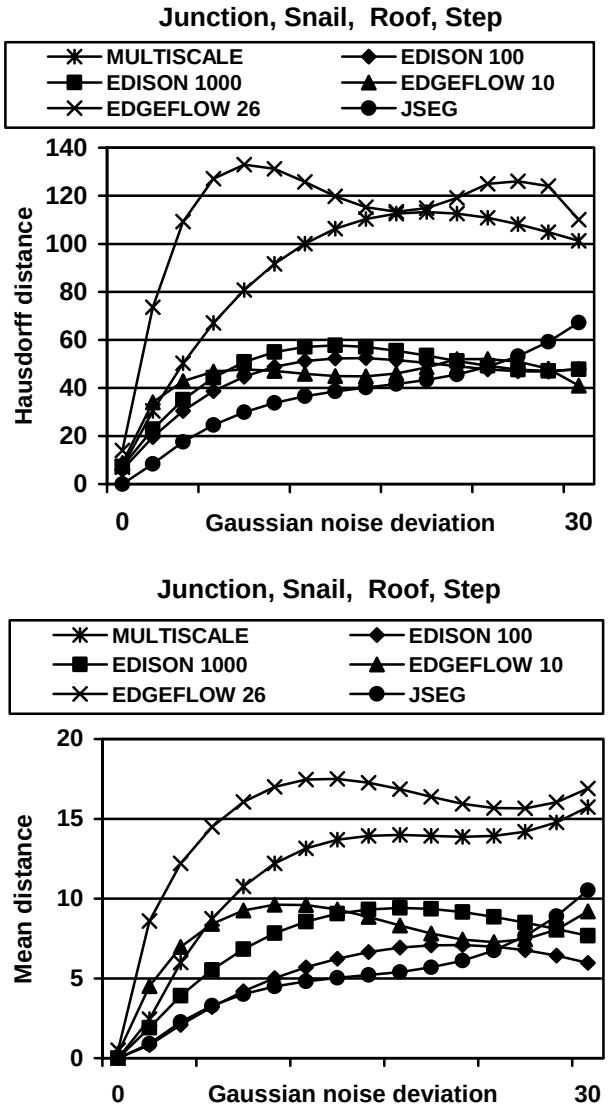

Fig.17. *Noisy images segmentation. Complex images. Averaged over Step, Junction, Snail and Roof images*

As to EDGEFLOW 10, the corresponding distances are smaller, but the plot starts to fall down approximately at the same noise deviation value.

MULTISCALE is slightly more stable to noise. However, high levels of χ and μ for this method indicate that higher values of noise deviation lead to a big number of junk segments. EDISON and JSEG segmentators displayed better results. The plot for EDISON starts to fall down for the values of σ equal to 15-20. The results for JSEG are better.

Comparing the plots on Fig.15 and 17, we see that JSEG exposes the best results for both types of test images. The results for EDISON are close. The estimates of the upper noise level for these two segmentators are also similar.

5.5 Segmentation of blurred images

To study the segmentation quality on blurred images, we take pictures on Fig.5,8 (simple images) and perform their Gaussian blurring with 0-12 pixel radius. Same as in the previous section, we also take pictures on Fig.9 (complex images) and perform their blurring with 0-3 pixel radius.

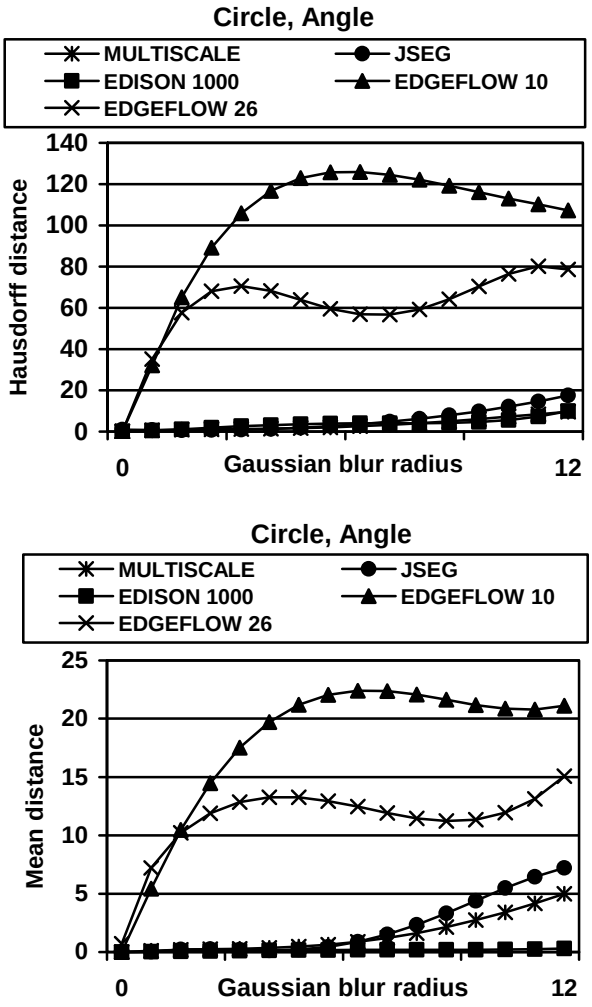

Fig.18. *Blurred images segmentation. Simple images. Averaged over Circle and Angle images*

Simple images. Fig.18 shows comparative results for all four methods applied to the blurred simple images. The plots for MULTISCALE and EDISON segmentators are almost identical.

EDISON displays the best quality: its distances χ and μ are smaller comparative to corresponding distances of all other methods. This means good shape preservation of the boundaries on the blurred image. As to the EDGEFLOW segmentator, we conclude that it can work while the blur radius does not exceed 3-4 pixels. For greater values, it creates many junk segments on the segmentation map (high values of χ indicate to this fact). JSEG works well up to the blurring radius 8-9. MULTISCALE displays close results.

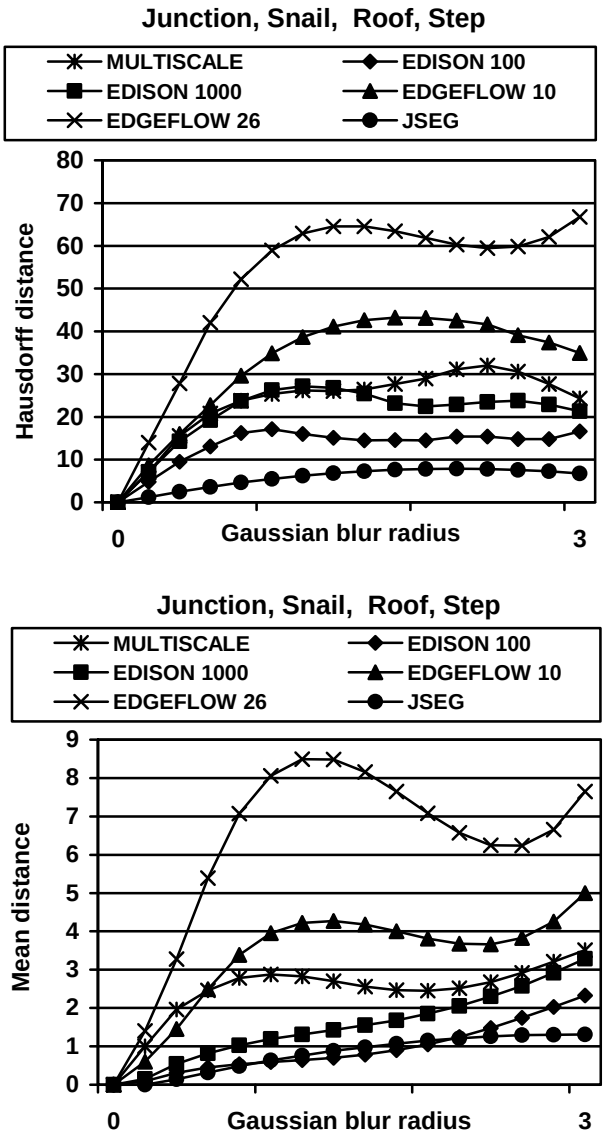

Fig.19. *Blurred images segmentation. Complex images. Averaged over Step, Junction, Snail and Roof images*

Complex images. Segmentation of these images proved to be a difficult task. Pay attention at the scales of horizontal axes on Fig.18,19. As we see, JSEG segmentator displays the best quality comparative to all other segmentators, since its distances χ and μ are the smallest. EDGEFLOW segmentator can work properly while the blur radius is not greater than 1-1.5 pixels. As χ is much greater than μ (Fig.19, then for bigger values of blur radius, the number of junk segments rapidly increases. Hausgorff distances are similar for EDISON 1000 and MULTISCALE segmentators. Their plots decrease for the values of blur radius greater than 2 pixels what means that the results of segmentation become almost arbitrary and improper.

6 Conclusions

According to basics of the PICASSO's ideology, we have modeled some typical and difficult situations in image segmentation. Using our set of artificial test images, one can detect some essential features of image segmentators.

As appeared, not all segmentators can well preserve the geometric form of objects on an image. For example, if an object contains an acute angle, some segmentators distort it.

Also, it appeared that one of the most essential problems of image segmentators is creation of "false boundaries" on images with slowly varying intensity (brightness). Thus the development of new computer programs which could minimize the amount of such boundaries would be a considerable contribution to the practice of image processing.

It turned out that segmentators have unstable behavior at processing of noisy and blurred images. That is, if an image is only slightly corrupted, the result of its segmentation can undergo considerable changes. Therefore, it is highly desirable to diminish noise and blur levels of images before their segmentation. Using our test images, it is possible to estimate the limits of applicability of segmentators.

References:

1. F. Meyer, C. Vachier. Image Segmentation Based On Viscous Flooding Simulation. *Proc. ISMM'02, CSIRO*, Sydney, Apr 2002, pp. 69–77.

2. Wei-Ying Ma and B. S. Manjunath. EdgeFlow: A Technique for Boundary Detection and Image Segmentation. *IEEE Transactions on Image Processing*, IEEE, Vol.9, Aug. 2000, pp. 1375-88

3. David Mumford. The Bayesian Rationale for Energy Functionals. *Geometry Driven Diffusion in Computer Vision*, Kluwer Academic, Dordrecht, The Netherlands, 1994, pp. 141–153.

4. Chen Zhuo, Francis Y.L. Chin and Ronald H.Y. Chung. Automated hierarchical image segmentation based on merging of quadrilaterals. *WSEAS Transactions on Signal Processing*, Vol. 2, No. 8, Aug. 2006, pp. 1063-1068.

5. *Zhengmao Ye, Jiecai Luo, Pradeep Bhattacharya, Yongmao Ye.* Segmentation of Aerial Images and Satellite Images Using Unsupervised Nonlinear Approach. *WSEAS Transactions on Systems*, Issue 2, Vol.5, Feb. 2006, pp. 333-340.

6. R. de Luis-García, C. Alberola-López. Hip joint segmentation for the diagnosis of developmental dysplasia of the hip using dynamic shape priors. *WSEAS Transactions on Signal Processing*2005, Vol. 3, No.1, pp. 432-438.

7. C.M.Christoudias, B.Georgescu, P.Meer: Synergism in low level vision. *16th International Conference on Pattern Recognition*., Quebec City, Canada, Aug. 2002, Vol. IV, pp. 150-155

8. B. Sumengen and B. S. Manjunath. Multi-scale Edge Detection and Image Segmentation. *Proc. European Signal Processing Conference (EUSIPCO)*, Sep. 2005. v: CD. Online. Available: http://vision.ece.ucsb.edu/publications/05eusipcoBarisMultiscale.pdf

9. Y.Deng and B.S.Manjunath. Unsupervised segmentation of color-texture regions in images and video. *IEEE Transactions on Pattern Analysis and Machine Intelligence (PAMI '01)*, Aug. 2001 Vol. 23, Issue: 8 pp. 800-810.

10. I.V.Gribkov, P.P.Koltsov, N.V.Kotovich, A.A.Kravchenko, A.S.Koutsaev, A.S.Osipov, A.V.Zakharov. Empirical Evaluation of Image Processing Methods Using PICASSO 2 System. *WSEAS Transactions on Systems*, Issue 11, Vol. 4, Nov. 2005, pp. 1923-1931.

11. I.V.Gribkov, P.P.Koltsov, N.V.Kotovich, A.A.Kravchenko, A.S.Koutsaev, A.S.Osipov, A.V.Zakharov. Edge detection under affine transformations: Comparative Study by the PICASSO 2 System. *WSEAS Transactions on Signal Processing*, Issue 9, Vol. 2, Sept. 2006, pp. 1215-1222.

12. Online. Available: http://vision.ece.ucsb.edu/segmentation/jseg/

13. Online. Available: http://www.caip.rutgers.edu/riul/research/code/EDISON/

14. Online. Available: http://vision.ece.ucsb.edu/segmentation/edgeflow

15. Online. Available: http://barissumengen.com/seg/